Methyl chloride variability in the Taylor Dome ice core during the Holocene

Kristal R. Verhulst,[1] Murat Aydin,[1] and Eric S. Saltzman[1]

Received 24 May 2013; revised 9 October 2013; accepted 10 October 2013; published 5 November 2013.

[1] Methyl chloride (CH_3Cl) is a naturally occurring, ozone-depleting trace gas and one of the most abundant chlorinated compounds in the atmosphere. CH_3Cl was measured in air from the Taylor Dome ice core in East Antarctica to reconstruct an atmospheric record for the Holocene (11–0 kyr B.P.) and part of the last glacial period (50–30 kyr B.P.). CH_3Cl variability throughout the Holocene is strikingly similar to that of atmospheric methane (CH_4), with higher levels in the early and late Holocene, and a well-defined minimum during mid-Holocene. The sources and sinks of atmospheric CH_3Cl and CH_4 are located primarily in the tropics, and variations in their atmospheric levels likely reflect changes in tropical conditions. CH_3Cl also appears to correlate with atmospheric CH_4 during the last glacial period (50–30 kyr B.P.), although the temporal resolution of sampling is limited. The Taylor Dome data provide information about the range of natural variability of atmospheric CH_3Cl and place a new constraint on the causes of past CH_4 variability.

Citation: Verhulst, K. R., M. Aydin, and E. S. Saltzman (2013), Methyl chloride variability in the Taylor Dome ice core during the Holocene, *J. Geophys. Res. Atmos.*, *118*, 12,218–12,228, doi:10.1002/2013JD020197.

1. Introduction

[2] Methyl chloride is the most abundant naturally occurring halocarbon gas in the atmosphere, with a global mean level of 550 ± 30 pmol mol^{-1} and an atmospheric lifetime of about 1 year. Currently, CH_3Cl comprises about 16% of the stratospheric chlorine burden. Future stratospheric ozone projections generally assume constant atmospheric CH_3Cl because there is little basis on which to predict future changes [*Montzka and Reimann*, 2010].

[3] Atmospheric measurements, field and laboratory flux studies, and atmospheric models estimate global CH_3Cl emissions to be approximately 4.1 to 4.4 Tg yr^{-1} [*Montzka and Reimann*, 2010; *Xiao et al.*, 2010]. The largest sources and sinks are located primarily in the tropics, based on latitudinal patterns in atmospheric CH_3Cl abundance [*Yoshida et al.*, 2004; *Xiao et al.*, 2010]. Terrestrial emissions are the dominant CH_3Cl sources and include direct biogenic emissions from vascular plants, abiotic release from leaf litter, and biomass burning of tropical forests, savannahs and grasslands [*Yokouchi et al.*, 2002; *Xiao et al.*, 2010]. Leaf litter CH_3Cl emissions arise from an abiotic chemical reaction between Cl^- and methoxy groups in plant pectin and exhibit a strong positive temperature dependence [*Hamilton et al.*, 2003; *Derendorp et al.*, 2012]. Emissions of CH_3Cl from temperate and subtropical ecosystems have also been observed but comprise a relatively small fraction of the total budget [*Varner et al.*, 1999; *Rhew et al.*, 2000; *Rhew*, 2011]. On a global scale, the oceans are a relatively small net source in the atmospheric CH_3Cl budget. Warm oceans are generally supersaturated with respect to the atmosphere and act as a CH_3Cl source, while the polar oceans are undersaturated and act as a sink [*Moore et al.*, 1996]. The major atmospheric loss pathway of CH_3Cl is oxidation by hydroxyl radical (OH). Other loss processes include microbial degradation in soils, loss to the oceans, and loss to the stratosphere [*Yoshida et al.*, 2004]. The environmental factors controlling CH_3Cl emissions from various ecosystems remain poorly understood because there have been few field process studies.

[4] Measurements in firn air and shallow ice cores suggest that atmospheric CH_3Cl is preserved in the Antarctic ice archive [*Butler et al.*, 1999; *Aydin et al.*, 2004; *Williams et al.*, 2007]. The data from these studies suggest atmospheric CH_3Cl levels increased by roughly 10% during the twentieth century, and climate-related variations of similar magnitude also occurred over the past millennium. There are limited CH_3Cl measurements from deep Antarctic ice cores (Dome Fuji and Siple Dome, Antarctica) showing some evidence of post-depositional CH_3Cl enrichment, particularly in ice with high dust content from the last glacial period and glacial/interglacial transition [*Saito et al.*, 2007; *Saltzman et al.*, 2009]. *Saito et al.* [2007] showed that elevated calcium levels (a proxy for dust) are a possible indicator of in situ production of CH_3Cl using ice core samples from the Dome Fuji ice core.

Additional supporting information may be found in the online version of this article.

[1]Department of Earth System Science, University of California, Irvine, California, USA.

Corresponding author: K. R. Verhulst, Department of Earth System Science, University of California, Irvine, 1212 Croul Hall, Irvine, CA 92697, USA. (k.verhulst@uci.edu)

2169-897X/13/10.1002/2013JD020197

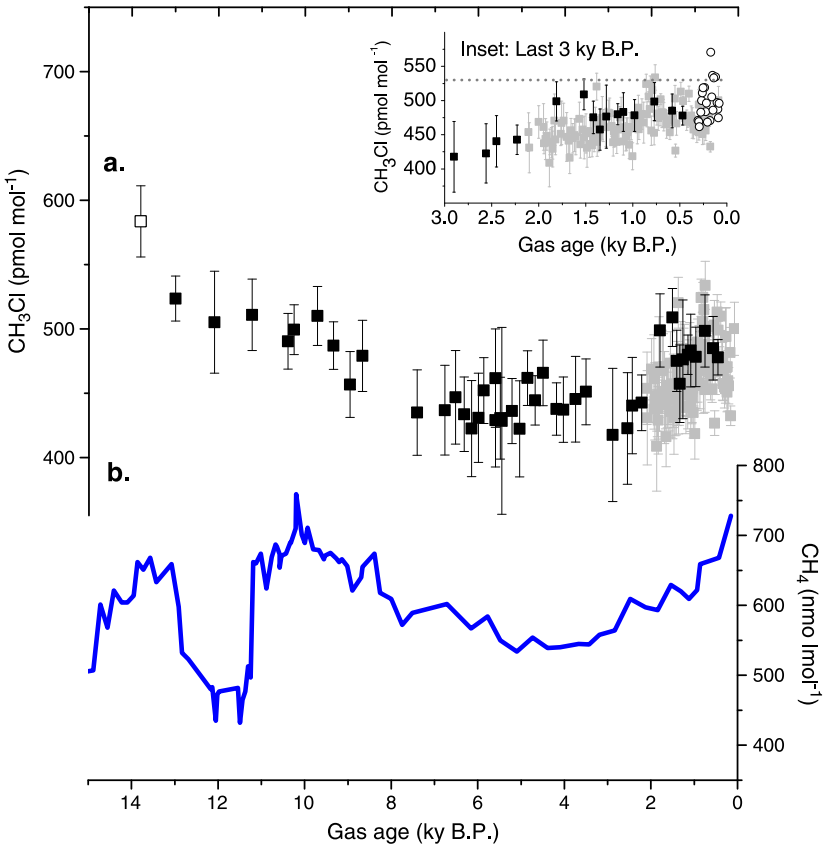

Figure 1. (a) Atmospheric history of CH_3Cl during the Holocene from the Taylor Dome (black squares, this study) and South Pole ice cores (gray squares) [*Williams et al.*, 2007]. All data are plotted with $\pm 1\sigma$ errors. The open square at 13.8 kyr B.P. is a Taylor Dome sample with calcium above 0.25 μM (see text). (inset) Comparison of Taylor Dome CH_3Cl measurements covering the last 3000 years (black squares, this study) with prior shallow ice core measurements from South Pole (filled grey squares) and Siple Dome C (open circles) [*Williams et al.*, 2007; *Aydin et al.*, 2004]. Dashed line represents modern-day mean level over Antarctica (~530 pmol mol^{-1}) [*Aydin et al.*, 2004]. (b) Atmospheric history of CH_4 from Taylor Dome [*Brook et al.*, 2000].

[5] Given our current understanding of the processes controlling atmospheric CH_3Cl today, we expect that CH_3Cl levels in the ancient atmosphere were sensitive to changes in tropical ecosystems and climate. A polar ice core based atmospheric history of CH_3Cl could provide a unique proxy signal that reflects changes in tropical conditions. Paleoatmospheric CH_3Cl levels might also reflect changes in atmospheric reactivity (i.e., global OH), and the interpretation of such a record requires disentangling the competing effects of changes in sources and sinks.

[6] In this study, we present measurements of CH_3Cl in air extracted from the Taylor Dome ice core. The data provide a record of CH_3Cl covering the Holocene (11–0 thousand years before 1950, kyr B.P.), with more limited coverage of the last glacial period between 50–30 kyr B.P. The Taylor Dome record provides new information about the range of natural CH_3Cl variability over glacial/interglacial timescales. The CH_3Cl data from Taylor Dome also exhibit a relationship to atmospheric CH_4, which has not been previously observed.

2. Ice Core Sampling, Analysis, and Dating

[7] Taylor Dome is a 554 m ice core that was recovered in East Antarctica between 1991 and 1994 (77°48′S, 158°43′E [*Steig et al.*, 2000]. Air was extracted from bubbles in ice core samples by mechanical shredding at –50°C under vacuum in an evacuated stainless steel chamber. The extracted air was collected in a stainless steel tube cooled with liquid helium (4K). Sample air was analyzed by gas chromatography with high-resolution mass spectrometry using an internal isotope-labeled gas standard calibrated against ppm-level primary gas standards. The apparatus and procedures used to extract and analyze gases from the ice core samples were similar to those used in earlier studies [*Saltzman et al.*, 2004; *Aydin et al.*, 2007; *Saltzman et al.*, 2009]. A correction of approximately –1% was applied to the measured CH_3Cl mixing ratios to account for gravitational enrichment in firn air, based on a bubble lock-in depth of 66 m and a mean annual surface air temperature of –42.5°C [*Craig et al.*, 1988]. Gas ages for the Holocene samples used in this study are based on stratigraphic correlation of the CO_2 record from Taylor Dome ice core to the European Project for Ice Coring in Antarctica (EPICA) Dome C and Dronning Maud Land ice cores [*Monnin et al.*, 2004]. Gas ages for the last glacial and transition samples are based on correlation of CO_2 and CH_4 records from Taylor Dome to the Greenland Ice Sheet Project 2 ice core [*Brook et al.*, 2000; *Ahn and Brook*, 2008] (see Table S1 in the supporting information).

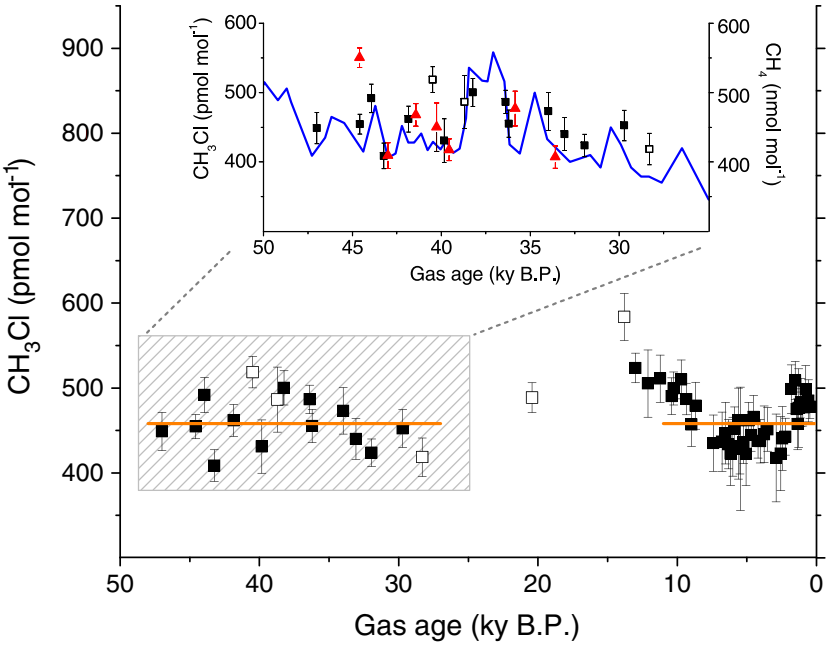

Figure 2. Methyl chloride measurements from the Taylor Dome ice core covering the last 50 kyr B.P. (black filled and open squares, left *y* axis). Orange lines represent the mean CH_3Cl level in samples from the last glacial period (50–30 kyr) and the Holocene (11–0 kyr). (inset) Enlarged view of the Taylor Dome CH_3Cl measurements from 50 to 25 kyr B.P., plotted with Siple Dome CH_3Cl measurements (red triangles) and atmospheric CH_4 levels from Taylor Dome (blue line, right *y* axis) [*Saltzman et al.*, 2009; *Brook et al.*, 2000]. Error bars in both panels represent $\pm 1\sigma$ errors of the CH_3Cl measurements. Open squares indicate Taylor Dome samples with calcium at or above 0.25 μM (see text).

[8] Methyl chloride analysis requires 400–600 g of high-quality ice, without fractures, and clean sampling, extraction, and analytical procedures. The aim of this study was to measure CH_3Cl in Taylor Dome ice core samples with equally spaced gas ages throughout the length of the core. However, ice samples of sufficient size/quality were limited for the last glacial period. As a result, the sample age distribution was heavily biased towards the Holocene. We analyzed 41 Taylor Dome ice core samples at 250–300 year intervals over the last 11 kyr B.P. and four additional samples from 15–11 kyr B.P. There were sampling gaps around 8 and 4 kyr B.P. due to lack of ice availability. In total, 94 ice core samples were analyzed. Data from only 62 samples were of sufficient quality for use in this study. Two samples were below the age-depth scale, and the remainder were considered poor quality due to (1) drill fluid contamination (n-butyl acetate), (2) modern air contamination (CFC-12 >1 pmol mol^{-1}), and (3) contamination of the extraction vessels [*Aydin et al.*, 2007, 2010] (see Figure S1). Methyl chloride levels in the samples ranged from 412 to 588 pmol mol^{-1}. The average analytical uncertainty was $6 \pm 2.6\%$ (1σ) of the measured levels.

2.1. Excess Methyl Chloride

[9] We examined calcium as a proxy for dust following *Saito et al.* [2007], using major ion data from *Mayewski et al.* [1996]. There is no correlation between Ca^{2+} and CH_3Cl in the Taylor Dome samples, suggesting there is no in situ production of methyl chloride (see Figure S2). In Siple Dome ice, there is evidence of "excess CH_3Cl" in samples with Ca^{2+} above 0.25 μM [*Saltzman et al.*, 2009]. Five measurements from the Taylor Dome ice core have Ca^{2+} at or above this level and are highlighted in Figures 1, 3, and S2. Holocene methyl chloride measurements from Siple Dome are elevated and scattered relative to Taylor Dome, even in samples with Ca^{2+} below 0.25 μM (Figure S2). This suggests that other site-specific properties may influence the CH_3Cl signal in Antarctic ice cores [*Saltzman et al.*, 2009].

3. Results

3.1. Holocene and Pre-Boreal Period (15–0 kyr B.P.)

[10] Methyl chloride variability during the Holocene ranges from about 418 to 515 pmol mol^{-1} (Figure 1a). Three measurements around the Younger Dryas/Pre-Boreal (YD/PB, about 13–11 ky B.P.) range from 509 to 527 pmol mol^{-1} and show little difference from Early Holocene mixing ratios. After 10 kyr B.P., CH_3Cl levels begin to decline, reaching a broad minimum during the mid-Holocene. The CH_3Cl minimum lasts from about 7.4 to 3.5 kyr B.P., with a mean level of 440 ± 14 pmol mol^{-1} (1σ SD, n = 21). At 3.5 kyr, CH_3Cl levels begin to increase and reach 480 pmol mol^{-1} at 0.5 kyr B.P.

[11] The Taylor Dome results from the Holocene can be validated by comparison to existing CH_3Cl measurements from Antarctic ice cores. The late Holocene CH_3Cl measurements overlap with prior measurements from the Siple Dome and South Pole shallow ice cores (see Figure 1 (inset)) [*Aydin et al.*, 2004; *Williams et al.*, 2007]. The Taylor Dome and South Pole time scales are independent, which

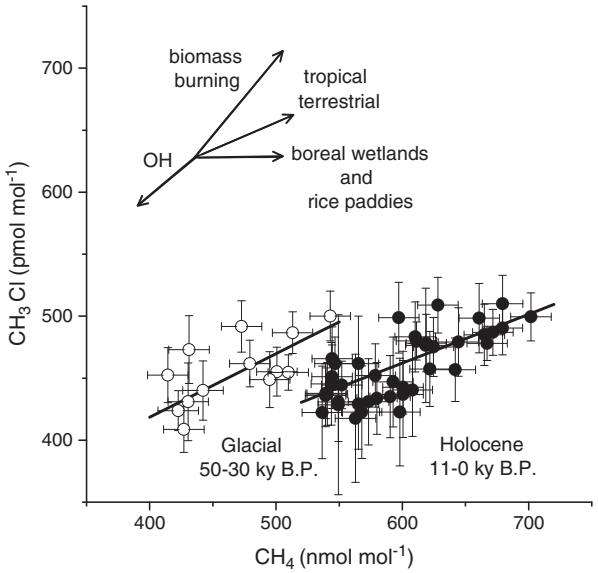

Figure 3. Taylor Dome CH_3Cl measurements from glacial (open circles) and Holocene (filled circles) samples plotted against CH_4 levels. CH_4 levels were determined at the CH_3Cl sample depths by linear interpolation of the Taylor Dome CH_4 record from *Brook et al.* [2000]. Three measurements around the Younger Dryas/Pre-Boreal are omitted. Black lines represent the slopes of Holocene and glacial samples. (inset) Lifetime-corrected CH_3Cl/CH_4 atmospheric response ratios calculated for various sources and sinks shared by the two trace gases using the preindustrial CH_4 and CH_3Cl lifetimes (see Table 2). The slope of the arrows reflects the change in the atmospheric CH_3Cl/CH_4 ratio that would result from an increase in various sources or sinks.

introduces uncertainty into the comparison of individual samples. Nonetheless, the Taylor Dome CH_3Cl measurements from the last 2 kyr have a mean level of 483.6 ± 14 (1σ SD) and agree well with South Pole data where sample ages overlap. The average rate of increase in Taylor Dome samples between 3.5 and 0.5 kyr B.P. is roughly 30 pmol mol^{-1}/1000 years, identical to the trend observed in the South Pole ice core from 2.2 to 0.2 kyr B.P. [*Williams et al.*, 2007] (see Figure 1 (inset)). The South Pole and Siple Dome C results also agree where the two cores overlap [*Williams et al.*, 2007]. The mean CH_3Cl level measured in Holocene samples from Taylor Dome is also similar to the Holocene mean measured in the Dome Fuji ice core (Figure S3) [*Saito et al.*, 2007]. The agreement between the new Taylor Dome data and prior South Pole measurements supports the idea that atmospheric CH_3Cl remains intact in the bubbles trapped in Antarctic ice cores and that these ice core measurements represent an atmospheric history of CH_3Cl.

3.2. Last Glacial Period (50–20 kyr B.P.)

[12] High-quality methyl chloride data were obtained in 17 samples with gas ages ranging from 50 to 20 kyr B.P. (Figure 2). Four of these samples exhibit elevated calcium levels, above 0.25 μM, as discussed earlier (see section 2 and Figure S2, supporting information). Taylor Dome data are similar to glacial CH_3Cl levels measured in the Siple Dome ice core (Figure 2). The mean of methyl chloride measurements from the last glacial period (50–30 kyr B.P.) is 456 ± 27 pmol mol^{-1} (1σ SD, $n = 13$). Methyl chloride levels measured in glacial ice samples are not statistically different from the interglacial levels ($t = 2.67$, $p = 0.01$, two-tailed Student's t test). *Saito et al.* [2007] found significantly higher CH_3Cl levels in glacial ice samples compared to the Holocene in the Dome Fuji ice core. The CH_3Cl enhancement was likely related to elevated impurity (dust) levels in the Dome Fuji ice core. The mean CH_3Cl level measured in glacial Taylor Dome samples is significantly lower than the glacial Dome Fuji measurements, even after the measurements were corrected for excess CH_3Cl production (Figure S3). This suggests that the in situ CH_3Cl enhancement in Dome Fuji ice is likely larger than previously estimated [*Saito et al.*, 2007].

3.3. Relationship to Methane

[13] Methyl chloride variability during the Holocene is strikingly similar to that of atmospheric CH_4 (Figure 1b). Both records exhibit a saddleback pattern with relative maxima in the early and late Holocene and a well-defined, contemporaneous minimum during the mid-Holocene. Methane levels decrease by roughly 20% from the early to mid-Holocene (from about 700 to 550 nmol mol^{-1}), while CH_3Cl levels decrease by about 10–15% over the same period (from about 490–500 pmol mol^{-1} in the early Holocene to 440 pmol mol^{-1} in the mid-Holocene). After 3.5 kyr, CH_3Cl and CH_4 rise by 11% and 19%, respectively, reaching their peak preindustrial levels (Figure 1).

[14] Measurements from the last glacial period show evidence of a similar relationship, with higher CH_3Cl levels during periods with elevated CH_4 levels (Figure 2 (inset)). Between 50 and 30 kyr B.P., CH_4 exhibits a baseline level between 400 and 450 nmol mol^{-1}, with positive excursions associated with interstadial warming events [*Chappellaz et al.*, 1993a; *Brook et al.*, 2000]. The CH_3Cl/CH_4 covariance is particularly notable within interstadial 8, around 38 kyr B.P.

[15] The relationship between CH_3Cl and CH_4 is shown in a regression plot (Figure 3, Table 1). To construct this plot, we linearly interpolated the Taylor Dome CH_4 data at the CH_3Cl depths. Regression fits are based on a weighted linear least squares regression with errors in both variables [*Reed*, 2010]. Eight measurements were excluded from the regression analyses: three from the YD/PB transition and five with the highest calcium levels (Figure S2). The YD is marked by a rapid drop in atmospheric CH_4. Interestingly, CH_3Cl levels show no change during the YD, based on a single CH_3Cl measurement around 12.1 kyr B.P. (Figure 1). Samples from the YD/PB period were excluded from the regression analyses due to the limited availability of samples.

Table 1. Regression Statistics for CH_3Cl and CH_4 Correlations in the Taylor Dome Ice Core (see Figure 3)[a]

Time Period (kyr B.P.)	Slope ± 2*s.e.	r	n
50–30	0.46 ± 0.25	0.66	13
11–0	0.39 ± 0.10	0.75	41
11–6	0.62 ± 0.11	0.96	12
3–0.5	1.13 ± 0.68	0.67	13

[a]Units for the slope are pmol mol^{-1} CH_3Cl/nmol mol^{-1} CH_4.

Table 2. Source Strengths, Emissions Ratios, and Lifetime-Corrected Atmospheric Response Ratios Calculated for Methyl Chloride and Methane (Figure 3 (inset))[a]

Source	CH_4 Emissions Tg y^{-1}	CH_3Cl Emissions Tg y^{-1}	Emission Ratio Tg CH_3Cl/ Tg CH_4	Atmospheric Response Ratio pmol mol^{-1} CH_3Cl/ nmol mol^{-1} CH_4
Boreal wetland	43.3	0.011	2.44×10^{-4}	0.01
Rice paddies	28.6	0.05	1.75×10^{-3}	0.08
Tropical wetland	151.3	0.037	2.44×10^{-4}	0.01
Tropical vegetation	–	2.2	–	–
Tropical terrestrial	151.3	2.237	1.48×10^{-2}	0.51 ± 0.1
Pyrogenic	23.5	0.917	3.9×10^{-2}	1.43 ± 0.3

[a]We assumed a preindustrial atmospheric lifetime of 6.9 years for CH_4 and 0.75 year for CH_3Cl. Emissions estimates are described in the supporting information. Tropical terrestrial emissions are the sum of emissions from tropical wetlands plus tropical vegetation.

[16] The slope of the Holocene and last glacial data are identical within their respective uncertainties, suggesting that the processes controlling atmospheric variability of these trace gases may not have been dramatically different under glacial and interglacial conditions (Figure 3). During the transition between the last glacial (50–30 kyr B.P.) and interglacial (11–0 kyr B.P.) periods, the mean CH_4 level increased by about 180 nmol mol^{-1} [*Brook et al.*, 2000], while the mean CH_3Cl level did not change. The shift from glacial to interglacial conditions likely affected the global budgets of these two gases differently.

3.4. Lifetime-Weighted Atmospheric Response Ratios

[17] We can estimate how changes in various sources influence the CH_3Cl/CH_4 ratio in the atmosphere by computing a lifetime-weighted atmospheric response ratio:

$$\frac{\partial CH_3Cl}{\partial CH_4}\left(\frac{\text{pmol/mol}}{\text{nmol/mol}}\right) = \frac{E_{CH_3Cl}}{E_{CH4}}\frac{\tau_{CH_4}}{\tau_{CH_3Cl}}\frac{16}{50.5} \times 10^3 \qquad (1)$$

where E_{CH3Cl} and E_{CH4} are the emissions of methyl chloride and methane, respectively, from a particular source (Tg y^{-1}), τ_{CH3Cl} and τ_{CH4} are the preindustrial atmospheric lifetimes of the two gases (0.75 year for CH_3Cl and 6.9 years for CH_4), and 16/50.5 is the ratio of the molecular weights.

[18] Lifetime-weighted atmospheric response ratios were calculated for various sources using information about the modern and preindustrial methane and methyl chloride budgets (Table 2). The CH_3Cl/CH_4 emissions ratio for tropical terrestrial sources was calculated using the sum of emissions from tropical wetlands and tropical vegetation [*Bergamaschi et al.*, 2007; *Xiao et al.*, 2010]. Based on these estimates, the lifetime-weighted atmospheric response ratio is 0.51 ± 0.1 pmol mol^{-1} CH_3Cl/nmol mol^{-1} CH_4 for tropical terrestrial emissions and 1.43 ± 0.3 pmol mol^{-1} CH_3Cl/nmol mol^{-1} CH_4 for pyrogenic emissions. The uncertainty estimates are based on the range and magnitude of CH_3Cl emissions from tropical plants and pyrogenic sources, respectively [*Xiao et al.*, 2010]. The calculations of tropical terrestrial CH_3Cl and CH_4 emissions are described in the supporting information. Atmospheric OH is the major loss pathway for both CH_4 and CH_3Cl. Therefore, a change in atmospheric OH results in a similar fractional change in steady state atmospheric CH_3Cl and CH_4 levels and an atmospheric response ratio near unity (Figure 3 (inset)).

[19] The slopes of the CH_3Cl versus CH_4 correlations for the Holocene and last glacial period are similar to the atmospheric response ratio from tropical terrestrial emissions (Figure 3). This is not surprising given that the major CH_3Cl sources are tropical. The slope of the CH_3Cl versus CH_4 regression is not compatible with changes due to biomass burning or boreal sources alone but could reflect the weighted sum of changes in multiple sources or in atmospheric OH. In contrast, the mean atmospheric CH_4 level increased between the glacial and interglacial periods without a corresponding increase in CH_3Cl levels. This points to a change in boreal sources as the primary cause for this shift. It is unlikely that rice paddy emissions play a major role, as they did not become significant until the late Holocene and are a relatively small part of the preindustrial CH_4 budget [*Zhou*, 2011]. Samples from the YD/PB transition were excluded from the regression analyses due to limited sample availability. The negative CH_4 excursion observed during the YD is not apparent in the CH_3Cl record (Figure 1). This could reflect changes in extratropical CH_4 sources during

Table 3. Parameters Used in the CH_3Cl Box Model[a]

Parameter	Symbol	Value	Reference
Mass of atmosphere (mol)	M	1.42×10^{20}	
Mean mixed layer depth (m)	z	75	
Surface area of the ocean (m^2)	A	361×10^{12}	
Mean air-sea exchange coefficient (m y^{-1})	K_w	1.5×10^3	
Henry's law constant (m^3 atm mol^{-1})	H	8.78×10^{-3}	*Moore et al.* [1995]
Mean diffusivity through thermocline (m^2y^{-1})	D_z	5.4×10^3	
In situ degradation rate (y^{-1})	k_d	25.55	*Tokarczyk et al.* [2003]
Mean "eddy degradation" rate (m y^{-1})	$K_{ed} = (D_z k_d)^{0.5}$	371.4	
Ocean production rate (mol CH_3Cl y^{-1})	P_o	7.68×10^{10}	see text

[a]Values are from *Butler* [1994] unless otherwise noted.

Table 4. Methyl Chloride Global Budget Terms Estimated for the Modern Atmosphere Using the CH_3Cl Box Model

Emissions	Gg yr^{-1}	Lifetime (y)
Vegetation and biomass burning	2596	
Ocean	500	
Anthropogenic	344[a]	
Total source	3440	
Losses		
OH		1.3
Ocean		3.8
Soil		16.4
Stratosphere		35
Total lifetime		1.16

[a]Anthropogenic CH_3Cl sources are estimated at 10% of the modern budget, based on prior firn air and shallow ice core studies [*Butler et al.*, 1999; *Aydin et al.*, 2004].

the YD that are not linked to CH_3Cl. Future studies should investigate the relationship between atmospheric CH_4 and CH_3Cl during the YD/PB period.

4. Modeling

[20] Simple steady state global box models of CH_3Cl and CH_4 were used to explore the sensitivity of Holocene CH_3Cl levels to changes in emissions and atmospheric lifetime. In the modern atmosphere, the CH_3Cl interhemispheric gradient is negligible. Pole-to-equator gradients are only about 5% because most of the sources and sinks are located in the tropics [*Yoshida et al.*, 2004]. Currently, there is no information about paleo-interhemispheric CH_3Cl gradients. Future studies utilizing both Greenland and Antarctic ice cores could provide such information and allow more sophisticated model treatments. By comparing ice core data and model simulations, we make the implicit assumption that latitudinal CH_3Cl gradients did not change.

4.1. Methyl Chloride Box Model

[21] A box model is used to compute the global steady state atmospheric abundance of methyl chloride based on prescribed, time-varying emissions histories. The atmosphere is coupled to the global ocean, also represented by a single box, where the net oceanic flux of CH_3Cl varies as a function of the atmospheric level. Since CH_3Cl is both produced and consumed in the ocean, the oceanic CH_3Cl flux will oppose changes in the atmospheric mixing ratio, resulting in a negative feedback or "buffering" effect on atmospheric CH_3Cl levels caused by changes in other sources or sinks [*Butler*, 1994; *Yvon and Butler*, 1996]. This model was first developed by *Butler* [1994] for methyl bromide, and we use the same notation here. The mass balance equations for the coupled ocean-atmosphere CH_3Cl model are

$$\frac{dM_a}{dt} = S_{terr} + F_{oa} - F_l = 0 \quad (2)$$

$$\frac{dM_o}{dt} = P_o - F_{oa} - F_d - F_{ed} = 0 \quad (3)$$

where M_a and M_o are the burden of CH_3Cl in the atmosphere and surface ocean (mol). All other terms in equations (2) and (3) are fluxes (mol y^{-1}). In equation (2), S_{terr} is the sum of terrestrial sources, including biomass burning and vegetative emissions, F_{oa} is the net exchange across the air/sea interface, and F_l is the atmospheric loss of CH_3Cl due to OH, stratosphere, and soils. In equation (3), P_o is the oceanic production of CH_3Cl, F_d is the aquatic degradation rate of CH_3Cl, and F_{ed} is the loss rate from downward vertical mixing and chemical or biological degradation through the thermocline.

[22] The mass balance equations for the coupled ocean-atmosphere model are parameterized as follows:

$$\frac{dM_a}{dt} = S_{terr} + \frac{K_w A}{H}(p_w - p_a) - (k_{OH} + k_{soil} + k_{strat})p_a M \quad (4)$$

$$\frac{dM_o}{dt} = P_o - \frac{K_w A}{H}(p_w - p_a) - k_d M_o - \frac{K_{ed}}{z} M_o \quad (5)$$

where K_w is the mean air-sea exchange coefficient, A is the surface area of the ocean, H is the Henry's law constant [*Moore et al.*, 1995], p_w is the partial pressure of CH_3Cl in the water (atm), p_a is the partial pressure of CH_3Cl in the atmosphere at sea level (atm), k_{OH}, k_{soil}, and k_{strat} are the first-order loss rate constants for reaction with OH, soil degradation, and loss to the stratosphere, M is the total mass of the atmosphere, k_d is the psuedo-first-order loss constant for aquatic degradation in the surface layer, K_{ed} is the downward removal of CH_3Cl from the surface ocean by mixing, and z is the thickness of the surface layer [*Butler*, 1994]. Equations (4) and (5) are solved simultaneously using the parameter values listed in Table 3.

[23] Source and sink strengths used to estimate the modern atmospheric CH_3Cl level in the model are consistent with current estimates (Table 4) [*Xiao et al.*, 2010]. Terrestrial vegetative and biomass-burning emissions are treated as a single-budget term in the box model. The global oceanic production rate (P_o) of 7.68×10^{10} mol CH_3Cl y^{-1} was tuned to give a net ocean flux of 500 Gg y^{-1} using the source and sink strengths listed in Table 4. This oceanic production rate gives an oceanic CH_3Cl concentration of 81 pM and a partial atmospheric CH_3Cl lifetime with respect to the oceans of 3.8 y, consistent with current estimates [*Moore et al.*, 1996; *Tokarczyk et al.*, 2003]. We use a partial atmospheric CH_3Cl lifetime with respect to soil uptake based on *Yoshida et al.* [2004].

4.2. Methane Box Model

[24] The CH_3Cl model is also coupled to a CH_4 box model to explore the relationship between atmospheric CH_3Cl and CH_4 and to quantify changes in the atmospheric lifetimes of the two trace gases. The CH_4 box model is used to compute the steady state atmospheric CH_4 burden using the following equation:

$$M_{CH_4} = \frac{S}{k_{OH} + k_{soil} + k_{strat}} \quad (6)$$

where M_{CH_4} is the atmospheric CH_4 burden (mol), S is the total CH_4 source, and k_{OH}, k_{soil}, and k_{strat} are the first-order loss rate constants for reaction with OH, loss to the stratosphere, and soil uptake. Oceanic CH_4 emissions are relatively small and are assumed to be constant.

[25] Methane is also a major sink for OH and, as a result, the OH lifetime of methane is a related to the atmospheric

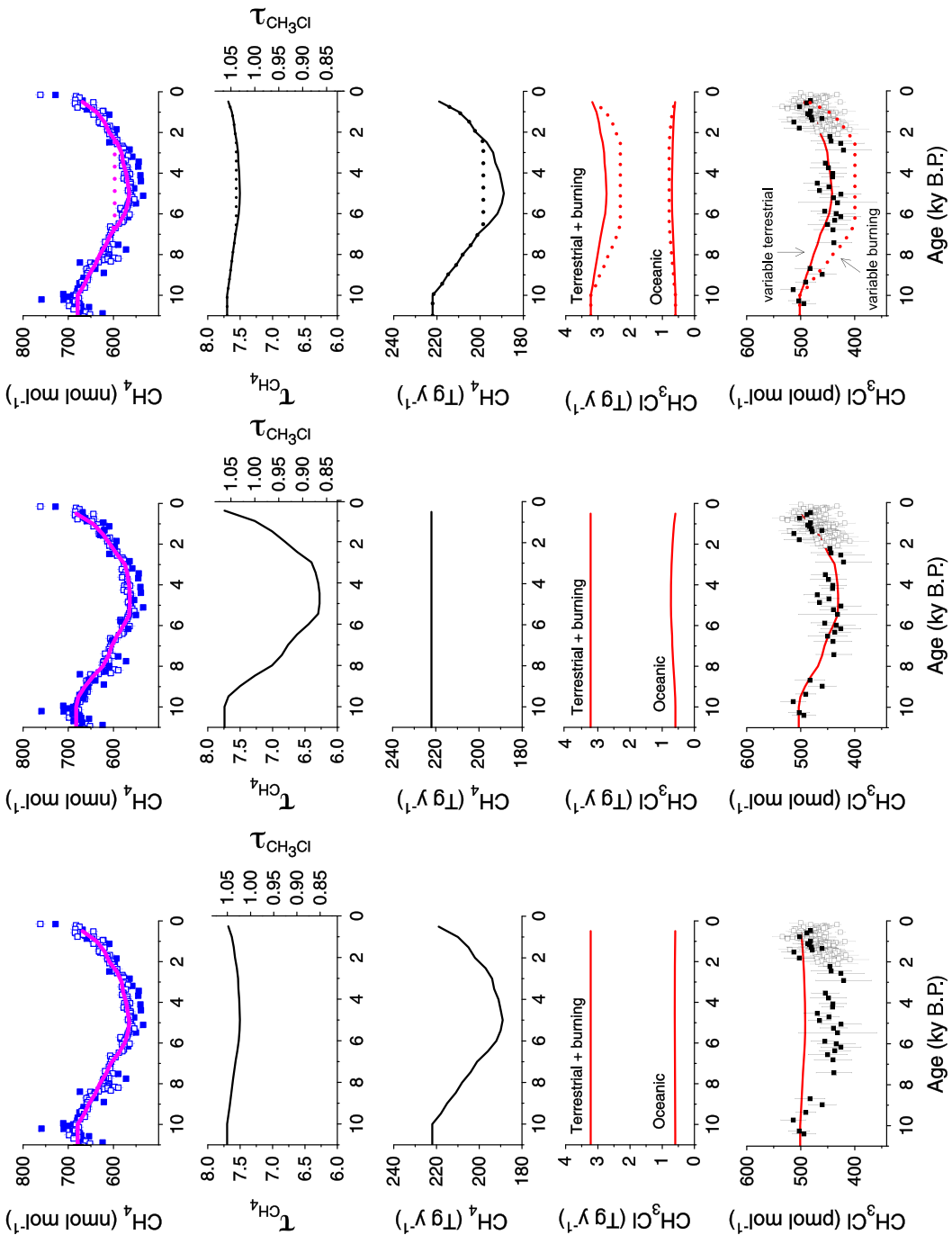

Figure 4. (left column) Model Scenario 1: Base Case results using variable CH_4 emissions, OH-methane feedback, and fixed terrestrial CH_3Cl emissions. (middle column) Model Scenario 2: OH-only results using fixed CH_4 emissions, fixed terrestrial CH_3Cl emissions, and variable OH lifetimes for CH_4 and CH_3Cl. (right column) Model Scenario 3: Fixed emissions ratio results using prescribed terrestrial CH_4 emissions, OH-methane feedback, and a fixed CH_3Cl/CH_4 ratio for tropical terrestrial emissions (solid lines) and biomass-burning emissions (dashed lines). (from top to bottom rows) Modeled atmospheric CH_4 (magenta line) and Taylor Dome and EPICA Dome C ice core data (filled and open blue squares) [*Brook et al.*, 2000; *Flückiger et al.*, 2002], partial atmospheric lifetimes with respect to OH for CH_4 (left y axis) and CH_3Cl (right y axis), prescribed total CH_4 emissions, terrestial and oceanic CH_3Cl emissions, and modeled atmospheric CH_3Cl (red line) and ice core data from Taylor Dome (black squares) and South Pole (open squares) [*Williams et al.*, 2007].

methane burden. The following expression is used to calculate changes in atmospheric CH_4 lifetime taking into account the methane feedback on atmospheric OH:

$$k_{OH+CH_4} = \frac{k^*_{OH+CH_4}}{\left(1 - \frac{\partial \ln OH}{\partial \ln CH_4} R\right)} \quad (7)$$

where

$$R = \frac{M_{CH_4} - M^*_{CH_4}}{M^*_{CH_4}} \quad (8)$$

and $\partial \ln OH / \partial \ln CH_4$ is the magnitude of the CH_4 feedback on atmospheric OH, $k^*_{OH+CH_4}$ is the present-day first-order loss rate constant for reaction of CH_4 with OH, and $M^*_{CH_4}$ is the modern atmospheric CH_4 burden. We use $k^*_{OH+CH_4} = (1/9.6)\ y^{-1}$ and $M^*_{CH_4}$=251 Tmol CH_4 (equivalent to 1774 nmol mol^{-1}) as conditions for the modern atmosphere [*Denman et al.*, 2007]. The magnitude of the CH_4 feedback on OH is taken as $\partial \ln OH / \partial \ln CH_4 = -0.32$, based on *Ehhalt et al.* [2001]. The steady state CH_4 burden and atmospheric lifetime are calculated by solving the equations (6)–(8) iteratively using the Matlab fsolve function.

[26] To couple the CH_3Cl and CH_4 box models, the OH lifetime of CH_3Cl is scaled to the OH lifetime of CH_4:

$$k_{OH+CH_3Cl} = \left(\frac{1.3}{9.6}\right) k_{OH+CH_4} \quad (9)$$

where k_{OH+CH_3Cl} and k_{OH+CH_4} are the first-order loss rate constants for loss of CH_3Cl and CH_4, and 1.3 and 9.6 are the modern OH lifetimes of CH_3Cl and CH_4, respectively.

4.3. Model Scenarios and Results

[27] Three model scenarios were examined using various assumptions about atmospheric lifetimes and the relationship between methyl chloride and methane emissions. In each case, emissions are specified at 0.5 kyr intervals from 11 to 0.5 kyr and the oceanic CH_3Cl production rate is held constant at the modern value. The simulation results are summarized in Figure 4.

[28] Scenario 1 (Base Case) examines the magnitude of changes in atmospheric CH_3Cl caused solely by the methane-OH feedback associated with the Holocene variations in atmospheric CH_4. For this model run, CH_4 emissions are specified to achieve agreement with data from the Taylor Dome and EPICA Dome C ice cores [*Brook et al.*, 2000; *Flückiger et al.*, 2002]. The CH_4 burden is calculated using equations (6)–(8), and equation (9) is used to scale the atmospheric OH lifetime of CH_3Cl. Terrestrial and biomass-burning CH_3Cl emissions are fixed at 3.2 Tg y^{-1}. The result from the base case scenario shows that the mid-Holocene increase in OH resulting from the CH_4 decrease alone accounts for about a 3% reduction in the atmospheric CH_3Cl abundance (Figure 4).

[29] Scenario 2 (OH-only) examines the question of whether the mid-Holocene minimum in both CH_4 and CH_3Cl could be caused by changes in atmospheric lifetimes alone. In this scenario, we impose fixed CH_3Cl and CH_4 emissions throughout the Holocene, with the exception of oceanic CH_3Cl emissions, which are based on a fixed oceanic production rate. The methane feedback on OH is turned off ($\partial \ln OH / \partial \ln CH_4 = 0$). The OH lifetime of CH_4 is specified in order to match the Holocene ice core CH_4 data, and equation (9) is used to scale the atmospheric OH lifetime of CH_3Cl. This simulation shows that a 26% decrease in CH_4 lifetime from the early Holocene to the mid-Holocene minimum is required to match the ice core observations. Interestingly, a change in CH_3Cl lifetime of this magnitude also provides a good fit to the ice core observations (Figure 4).

[30] Scenario 3 (Fixed CH_3Cl/CH_4 Emissions Ratio) is where tropical terrestrial CH_3Cl and CH_4 emissions are coupled throughout the Holocene using a constant emission ratio. We estimate this ratio to be 2.237 Tg CH_3Cl/151.3 Tg CH_4 (see Table 2 and supporting information). Total CH_4 emissions are adjusted as in the Base Case scenario. The CH_4 burden is calculated using equations (6)–(8), and equation (9) is used to scale the atmospheric OH lifetime of CH_3Cl. Ocean buffering causes the net oceanic CH_3Cl flux during the mid-Holocene to increase by about 200 Gg y^{-1} relative to the modern value. Scenario 3 yields reasonable agreement with the ice core CH_3Cl data (Figure 4), suggesting that changes in tropical terrestrial emissions (excluding pyrogenic emissions) are a viable explanation for the CH_3Cl and CH_4 trends. We also explored the possibility of changing pyrogenic emissions as a cause for the CH_4 and CH_3Cl trends. Methane emissions were adjusted as described above, and a fixed biomass-burning emissions ratio (0.917 Tg CH_3Cl/23.5 Tg CH_4, Table 2) was used to calculate pyrogenic CH_3Cl emissions. In our model, biomass burning constitutes a larger fraction of the CH_3Cl budget compared to its fractional contribution in the CH_4 budget. This explains why eliminating the entire pyrogenic source is insufficient to match the atmospheric CH_4 minimum but slightly overestimates the CH_3Cl decline during the mid-Holocene (Figure 4). It appears unlikely that the entire CH_3Cl decline was due to a decrease in pyrogenic emissions alone, however, because a very large fraction of the total pyrogenic emissions must be removed in order to match the ice core observations.

5. Discussion

[31] The most notable aspect of the atmospheric CH_3Cl budget is the extent to which it is dominated by tropical sources. Current estimates suggest that 60–90% of the total CH_3Cl emissions are from tropical regions, with the largest contributions from terrestrial plants and decaying leaf litter [*Yoshida et al.*, 2004; *Montzka and Reimann*, 2010; *Xiao et al.*, 2010]. Photochemical losses due to OH are also located primarily within the tropics. Thus, it is highly likely that variations in tropical conditions are responsible for the observed variations in atmospheric methyl chloride.

[32] Like CH_3Cl, atmospheric CH_4 has large tropical terrestrial sources. The most important natural source of atmospheric CH_4 is anaerobic decomposition of organic material in wetlands. Together, tropical emissions from wetlands and biomass burning comprise roughly 30% of the sources in the modern CH_4 budget [*Bergamaschi et al.*, 2007] and likely accounted for greater than 60% of the sources during late preindustrial Holocene [*Chappellaz et al.*, 1993b]. The causes of atmospheric CH_4 variability over both centennial and millennial timescales have been extensively

debated [*Dällenbach et al.*, 2000; *Ruddiman*, 2003; *Valdes et al.*, 2005; *Levine et al.*, 2011; *Sapart et al.*, 2012]; however, changes in tropical emissions are generally thought to be the primary driver of CH_4 variations during the preindustrial Holocene [*Chappellaz et al.*, 1997; *Flückiger et al.*, 2002; *Harder et al.*, 2007]. Changes CH_4 production from tropical wetlands during the Holocene have been attributed to orbitally driven variations in tropical hydrology [*Singarayer et al.*, 2011; *Burns*, 2011; *Dykoski et al.*, 2005; *Wang et al.*, 2007].

[33] Changes in tropical hydrology could also impact the tropical sources of CH_3Cl. As demonstrated in model Scenario 3, both the Holocene CH_3Cl and CH_4 ice core data can be reasonably simulated by reducing tropical terrestrial emissions by roughly 15% from the early to mid-Holocene. Assuming that the CH_3Cl/CH_4 ratio of tropical terrestrial emissions remained constant, emissions decreased by about 0.5 Tg CH_3Cl y^{-1} and 33 Tg CH_4 y^{-1} from the early to mid-Holocene. It is unlikely that the entire CH_3Cl minimum was driven by a decrease in biomass-burning emissions alone. Biomass burning constitutes only about 23% of the modern CH_3Cl budget, with the majority of these emissions occurring in the tropics [*Xiao et al.*, 2010]. Most of the pyrogenic CH_3Cl emissions would have to be removed during the mid-Holocene in order to match the ice core results. Subtropical, temperate, and non-terrestrial CH_3Cl sources alone are also too small to explain the observed trend. However, it is possible that the CH_3Cl trend was driven by simultaneous changes in several smaller sources, such as biomass burning, oceans, and extratropical emissions. The CH_3Cl data argue against changes in boreal emissions or the introduction of rice agriculture as primary drivers of CH_4 variability during the Holocene [*Ruddiman*, 2003; *Sapart et al.*, 2012], because CH_3Cl emissions from these sources are negligible [*Lee-Taylor and Redeker*, 2005].

[34] Atmospheric OH is the major loss pathway for both CH_3Cl and CH_4. Variations in atmospheric OH could explain the observed Holocene trends of both trace gases. The result from model Scenario 2 shows that a 26% decrease in the atmospheric lifetimes of CH_4 and CH_3Cl is required to fit the ice core data. This is significantly larger than the change in OH expected from the methane-OH feedback alone (model Scenario 1). It is also larger than the change in OH predicted in paleoatmospheric simulations involving full photochemistry and other climate feedbacks (ozone, water vapor, nonmethane hydrocarbons) [*Martinerie et al.*, 1995; *Valdes et al.*, 2005; *Levine et al.*, 2011]. However, there are no observations that directly constrain paleo-OH, so this cannot be eliminated as a cause for the CH_3Cl and CH_4 trends.

[35] There is intriguing evidence in the glacial Taylor Dome data that CH_3Cl and CH_4 may be correlated during interstadial events (Figures 2–3). The glacial regression slope is similar to the atmospheric response ratio for tropical terrestrial emissions. Thus, it is possible that the emissions of both CH_3Cl and CH_4 were also influenced by low-latitude climatic and/or environmental changes during interstadial events [*Chappellaz et al.*, 1993a], rather than solely due to changes in the northern latitude (boreal) sources [*Dällenbach et al.*, 2000]. A high-resolution glacial methyl chloride record across several interstadial events is needed to confirm this relationship.

[36] Measurements from Taylor Dome show that the mean CH_3Cl level did not change between the last glacial (50–30 kyr B.P.) and interglacial (11–0 kyr B.P.) periods. Although CH_3Cl data are lacking for the last glacial maximum, the data suggest that the change in mean CH_4 level between the last glacial and interglacial period was not shared by CH_3Cl. This implies that most of the methane rise between the last glacial and interglacial period may have been due to increasing boreal emissions. This supports earlier suggestions, which attribute most of the CH_4 rise during the last glacial-interglacial transition to the expansion of high-latitude, boreal wetlands following the retreat of Northern Hemisphere ice sheets [*Chappellaz et al.*, 1993b].

6. Conclusions

[37] The Taylor Dome results show that significant natural variations in atmospheric CH_3Cl occurred during the Holocene and last glacial period. Methyl chloride variability during the Holocene is strikingly similar to that of atmospheric methane, suggesting a common control on the natural variability of both trace gases. Both CH_3Cl and CH_4 have significant tropical terrestrial sources and share a major sink in OH. The underlying ecological and physiological factors controlling terrestrial vegetative emissions of CH_3Cl are not well understood. There are also no direct observations to constrain past changes in atmospheric OH. This limits the extent to which we can interpret ice core CH_3Cl as a measure of past environmental change. However, ice core CH_3Cl measurements provide a uniquely tropical signal that is archived along with other well-dated paleo-proxies in the polar ice core record.

[38] During preindustrial times, CH_3Cl was likely the major precursor of stratospheric chlorine. The ice core data suggest that natural CH_3Cl variability was on the order of 15–20% during the preindustrial Holocene. This is small compared to the fourfold increase in equivalent effective stratospheric chlorine that occurred during the twentieth century due to the anthropogenic emissions of CFCs and other chlorinated compounds [*Montzka and Reimann*, 2010]. Future changes in atmospheric CH_3Cl will likely be influenced by both climate and land use changes, particularly in tropical regions, as well as changes in the reactivity of the atmosphere induced by human activities. As a result, the Holocene observations may represent a lower limit to the range of CH_3Cl variability that could be expected in the future.

[39] **Acknowledgments.** We thank the National Ice Core Laboratory for assistance in sampling the Taylor Dome ice core, P. Mayewski for calcium data, and Ed Brook for providing methane data, assistance with the Taylor Dome chronology, and helpful discussions which improved the manuscript. We would also like to thank two anonymous reviewers for their insightful comments which helped improve the manuscript. This research was funded by the National Science Foundation Antarctic Glaciology program under grants ANT-0636953, 1043780, 0839122. Partial funding for Open Access provided by the UCI Libraries Open Access Publishing Fund.

References

Ahn, J., and E. J. Brook (2008), Atmospheric CO_2 and climate on millennial time scales during the last glacial period, *Science*, *322*(5898), 83–85, doi:10.1126/science.1160832.

Aydin, M., E. S. Saltzman, W. J. De Bruyn, S. A. Montzka, J. H. Butler, and M. O. Battle (2004), Atmospheric variability of methyl chloride during the last 300 years from an Antarctic ice core and firn air, *Geophys. Res. Lett.*, *31*(2), L02109, doi:10.1029/2003GL018750.

Aydin, M., M. B. Williams, and E. S. Saltzman (2007), Feasibility of reconstructing paleoatmospheric records of selected alkanes, methyl halides, and sulfur gases from Greenland ice cores, *J. Geophys. Res.*, *112*(D7), 1–9, doi:10.1029/2006JD008027.

Aydin, M., et al. (2010), Post-coring entrapment of modern air in some shallow ice cores collected near the firn-ice transition: Evidence from CFC-12 measurements in Antarctic firn air and ice cores, *Atmos. Chem. Phys.*, *10*(11), 5135–5144, doi:10.5194/acp-10-5135-2010.

Bergamaschi, P., et al. (2007), Satellite chartography of atmospheric methane from SCIAMACHY on board ENVISAT: 2. Evaluation based on inverse model simulations, *J. Geophys. Res.*, *112*(D2), D02304, doi:10.1029/2006JD007268.

Brook, E. J., S. Harder, J. Severinghaus, E. J. Steig, and C. M. Sucher (2000), On the origin and timing of rapid changes in atmospheric methane during the last glacial period, *Glob. Biogeochem Cyc.*, *14*(2), 559–572.

Burns, S. J. (2011), Speleothem records of changes in tropical hydrology over the Holocene and possible implications for atmospheric methane, *Holocene*, *21*(5), 735–741, doi:10.1177/0959683611400194.

Butler, J. (1994), The potential role of the ocean in regulating atmospheric CH_3Br, *Geophys. Res. Lett.*, *21*(3), 185–188.

Butler, J. H., M. Battle, M. L. Bender, S. A. Montzka, A. D. Clarke, E. S. Saltzman, C. M. Sucher, J. P. Severinghaus, and J. W. Elkins (1999), A record of atmospheric halocarbons during the twentieth century from polar firn air, *Nature*, *399*(June), 749–755.

Chappellaz, J., T. Blunier, D. Raynaud, J. M. Barnola, J. Schwander, and B. Stauffer (1993a), Synchronous changes in atmospheric CH_4 and Greenland climate between 40 and 8 kyr BP, *Nature*, *366*, 443–445.

Chappellaz, J., I. Fung, and A. M. Thompson (1993b), The atmospheric CH_4 increase since the last glacial maximum (1). Source estimates, *Tellus*, *45B*, 228–241.

Chappellaz, J., T. Blunier, S. Kints, A. Dallenbach, J. M. Barnola, J. Schwander, D. Raynaud, and B. Stauffer (1997), Changes in the atmospheric CH_4 gradient between Greenland and Antarctica during the Holocene, *J. Geophys. Res.*, *102*(97), 15,987–15,997.

Craig, H., Y. Horibe, and T. Sowers (1988), Gravitational separation of gases and isotopes in polar ice caps, *Science*, *242*(4886), 1675–1678, doi:10.1126/science.242.4886.1675.

Dällenbach, A., T. Blunier, and J. Flückiger (2000), Changes in the atmospheric CH_4 gradient between Greenland and Antarctica during the last glacial and the transition to the Holocene, *Geophys. Res. Lett.*, *27*(7), 1005–1008.

Denman, K., et al. (2007), Couplings between changes in the climate system and biogeochemistry, in *Climate Change 2007: The Physical Science Basis. Contribution of Working Group I to the Fourth Assessment Report of the Intergovernmental Panel on Climate Change*, edited by S. Solomon et al., pp. 239–287, Cambridge Univ. Press, Cambridge and New York.

Derendorp, L., A. Wishkerman, F. Keppler, C. McRoberts, R. Holzinger, and T. Röckmann (2012), Methyl chloride emissions from halophyte leaf litter: Dependence on temperature and chloride content, *Chemosphere*, *87*(5), 483–489, doi:10.1016/j.chemosphere.2011.12.035.

Dykoski, C., R. Edwards, H. Cheng, D. Yuan, Y. Cai, M. Zhang, Y. Lin, J. Qing, Z. An, and J. Revenaugh (2005), A high-resolution, absolute-dated Holocene and deglacial Asian monsoon record from Dongge Cave, China, *Earth and Plan. Sci. Lett.*, *233*(1-2), 71–86, doi:10.1016/j.epsl.2005.01.036.

Ehhalt, D., et al. (2001), Atmospheric chemistry and greenhouse gases, in *Climate Change 2001: The Physical Science Basis. Contribution of Working Group I to the Third Assessment Report of the Intergovernmental Panel on Climate Change*, edited by F. Joos, and M. McFarlan, pp. 241–287, Cambridge Univ. Press, Cambridge and New York.

Flückiger, J., E. Monnin, and B. Stauffer (2002), High-resolution Holocene N_2O ice core record and its relationship with CH_4 and CO_2, *Glob. Biogeochem. Cyc.*, *16*(1), 1010.

Hamilton, J. T. G., W. C. McRoberts, F. Keppler, R. M. Kalin, and D. B. Harper (2003), Chloride methylation by plant pectin: An efficient environmentally significant process, *Science*, *301*(5630), 206–209, doi:10.1126/science.1085036.

Harder, S. L., D. T. Shindell, G. a. Schmidt, and E. J. Brook (2007), A global climate model study of CH_4 emissions during the Holocene and glacial-interglacial transitions constrained by ice core data, *Global Biogeochem. Cycles*, *21*(1), GB1011, doi:10.1029/2005GB002680.

Lee-Taylor, J., and K. R. Redeker (2005), Reevaluation of global emissions from rice paddies of methyl iodide and other species, *Geophys. Res. Lett.*, *32*(15), L15801, doi:10.1029/2005GL022918.

Levine, J. G., E. W. Wolff, A. E. Jones, L. C. Sime, P. J. Valdes, A. T. Archibald, G. D. Carver, N. J. Warwick, and J. A. Pyle (2011), Reconciling the changes in atmospheric methane sources and sinks between the last glacial maximum and the pre-industrial era, *Geophys. Res. Lett.*, *38*(23), 2–7, doi:10.1029/2011GL049545.

Martinerie, P., G. Brasseur, and C. Granier (1995), The chemical composition of ancient atmospheres: A model study constrained by ice core data, *J. Geophys. Res.*, *100*(D7), 14,291–14,304.

Mayewski, P., et al. (1996), Climate change during the last deglaciation in Antarctica, *Science*, *272*, 1636–1638.

Monnin, E., et al. (2004), Evidence for substantial accumulation rate variability in Antarctica during the Holocene, through synchronization of CO_2 in the Taylor Dome, Dome C and DML ice cores, *Earth and Plan. Sci. Lett.*, *224*(1-2), 45–54, doi:10.1016/j.epsl.2004.05.007.

Montzka, S. A., and S. Reimann (2010), Ozone-Depleting Substances and Related Chemicals, in Scientific Assessment of Ozone Depletion: 2010, Global Ozone Research and Monitoring Project, Tech. rep., World Meteorol Org., Geneva.

Moore, R., C. Geen, and V. Tait (1995), Determination of Henry's Law constants for a suite of naturally occurring halogenated methanes in seawater, *Chemosphere*, *30*(6), 1183–1191.

Moore, R. M., W. Groszko, and S. J. Niven (1996), Ocean-atmosphere exchange of methyl chloride: Results from NW atlantic and pacific ocean studies, *J. Geophys. Res.*, *101*(C12), 529–538.

Reed, B. C. (2010), A spreadsheet for linear least-squares fitting with errors in both coordinates, *Phys. Educ.*, *45*(1), 93–96, doi:10.1088/0031-9120/45/1/011.

Rhew, R. C. (2011), Sources and sinks of methyl bromide and methyl chloride in the tallgrass prairie: Applying a stable isotope tracer technique over highly variable gross fluxes, *J. Geophys. Res.*, *116*(G3), G03026, doi:10.1029/2011JG001704.

Rhew, R. C., B. R. Miller, and R. F. Weiss (2000), Natural methyl bromide and methyl chloride emissions from coastal salt marshes, *Nature*, *403*(6767), 292–295, doi:10.1038/35002043.

Ruddiman, W. (2003), The anthropogenic greenhouse era began thousands of years ago, *Clim. Change*, *61*, 261–293.

Saito, T., Y. Yokouchi, S. Aoki, T. Nakazawa, Y. Fujii, and O. Watanabe (2007), Ice-core record of methyl chloride over the last glacial Holocene climate change, *Geophys. Res. Lett.*, *34*(3), L03801, doi:10.1029/2006GL028090.

Saltzman, E. S., M. Aydin, W. J. De Bruyn, D. B. King, and S. A. Yvon-Lewis (2004), Methyl bromide in preindustrial air: Measurements from an Antarctic ice core, *J. Geophys. Res.*, *109*(D5), D05301, doi:10.1029/2003JD004157.

Saltzman, E. S., M. Aydin, M. B. Williams, K. R. Verhulst, and B. Gun (2009), Methyl chloride in a deep ice core from Siple Dome, Antarctica, *Geophys. Res. Lett.*, *36*(3), L03822, doi:10.1029/2008GL036266.

Sapart, C. J., et al. (2012), Natural and anthropogenic variations in methane sources during the past two millennia, *Nature*, *490*(7418), 85–88, doi:10.1038/nature11461.

Singarayer, J. S., P. J. Valdes, P. Friedlingstein, S. Nelson, and D. J. Beerling (2011), Late Holocene methane rise caused by orbitally controlled increase in tropical sources, *Nature*, *470*(7332), 82–85, doi:10.1038/nature09739.

Steig, E., D. Morse, E. Waddington, M. Stuiver, P. Grootes, P. Mayewski, M. Twickler, and S. Whitlow (2000), Wisconsinan and Holocene climate history from an ice core at Taylor Dome, Western Ross Embayment, Antarctica, *Geogr. Ann.*, *82A*, 213–235.

Tokarczyk, R., E. S. Saltzman, R. M. Moore, and S. A. Yvon-Lewis (2003), Biological degradation of methyl chloride in coastal seawater, *Glob. Biogeochem Cyc.*, *17*(2), 735–741, doi:10.1029/2002GB001949.

Valdes, P. J., D. J. Beerling, and C. E. Johnson (2005), The ice age methane budget, *Geophys. Res. Lett.*, *32*(2), L02704, doi:10.1029/2004GL021004.

Varner, R. K., P. M. Crill, and R. W. Talbot (1999), Wetlands: A potentially significant source of atmospheric methyl bromide and methyl chloride, *Geophys. Res. Lett.*, *26*(16), 2433–2435.

Wang, X., A. S. Auler, R. L. Edwards, H. Cheng, E. Ito, Y. Wang, X. Kong, and M. Solheid (2007), Millennial-scale precipitation changes in southern Brazil over the past 90,000 years, *Geophys. Res. Lett.*, *34*(23), L23701, doi:10.1029/2007GL031149.

Williams, M. B., M. Aydin, C. Tatum, and E. S. Saltzman (2007), A 2000 year atmospheric history of methyl chloride from a South Pole ice core: Evidence for climate-controlled variability, *Geophys. Res. Lett.*, *34*(7), L07811, doi:10.1029/2006GL029142.

Xiao, X., et al. (2010), Optimal estimation of the surface fluxes of methyl chloride using a 3-D global chemical transport model, *Atmos. Chem. Phys.*, *10*(12), 5515–5533, doi:10.5194/acp-10-5515-2010.

Yokouchi, Y., M. Ikeda, Y. Inuzuka, and T. Yukawa (2002), Strong emission of methyl chloride from tropical plants, *Nature*, *416*(6877), 163–165, doi:10.1038/416163a.

Yoshida, Y., Y. Wang, and T. Zeng (2004), A three-dimensional global model study of atmospheric methyl chloride budget and distributions, *J. Geophys. Res.*, *109*(D24), D24309, doi:10.1029/2004JD004951.

Yvon, S., and J. Butler (1996), An improved estimate of the ocean lifetime of atmospheric CH_3Br, *Geophys. Res. Lett.*, *23*(1), 53–56.

Zhou, X. (2011), Asian monsoon precipitation changes and the Holocene methane anomaly, *Holocene*, *22*(7), 731–738, doi:10.1177/0959683611430408.